Theoretical Studies of the Ground and Excited Electronic States in Cyclometalated Phenylpyridine Ir(III) Complexes Using Density Functional Theory

P. Jeffrey Hay*

Theoretical Division, MS B268, Los Alamos National Laboratory, Los Alamos, New Mexico 87545

Received: October 25, 2001; In Final Form: December 19, 2001

The ground state and low-lying excited electronic states in the Ir(III) complex Ir(ppy)$_3$, and in the related complexes Ir(ppy)$_2$(acac) and Ir(ppy)$_2$(bza), are studied using density functional theory techniques [where ppy = 2-phenylpyridine, acac = acetoylacetonate, and bza = benzyolacetonate]. Ir complexes of ppy have been the subject of numerous photophysical absorption and luminescence experiments and have been examined as potential donors in organic light emitting diodes (OLEDs). The electronic properties of the neutral molecules, in addition to the positive and negative ions, are studied using the B3LYP functional. Optimized geometries are compared to experimentally observed structures. Excited triplet and singlet states are examined using time-dependent density functional theory (TDDFT). The calculated energies of the lowest triplet state (2.4−2.6 eV) and lowest singlet state (2.6−2.7 eV) in the three complexes are in good agreement with experimental absorption spectra and luminescence studies. All of the low-lying transitions are categorized as metal-to-ligand charge-transfer (MLCT) transitions. The metal orbitals involved in the transitions have a significant admixture of ligand π character, as shown by the amount of metal 5d character which varies from 45 to 65%. The nature of the lowest unoccupied orbital changes from ppy-localized to bza-localized for the series of three molecules.

Introduction

The photophysical properties of transition metal complexes, especially the d^6 Ru(II), Os(II), Rh(III,) and Ir(III) species, have been studied by a wide variety of spectroscopic and electrochemical techniques.[1−4] There remain many interesting questions regarding the nature of these states and the dynamic processes involved. In particular absorption spectra and emissive properties of Ir(ppy)$_3$ and related Ir(III) complexes, where ppy = 2-phenylpyridine, have been extensively studied in solution and in solid state.[5−15] Recently, Ir(ppy)$_3$ and related complexes have received attention as efficient phosphor dopants in polymer matrixes for applications as organic light emitting diode devices (OLEDs).[16−21]

The large size of the ligands and the significant role of correlation and relativistic effects have presented challenges to theoretical approaches to excited states of transition metal complexes. Configuration interaction based techniques such as CASSCF-MP2[22] have been applied to a variety of complexes, such as metal carbonyls,[23,24] as well as to Pd(thpy)$_2$ and Pt-(thpy)$_2$.[25] In recent years, approaches using density functional theory (DFT) have received large acceptance for describing the ground state properties of organometallic and inorganic molecules. Remarkable structural and thermochemical predictions have been obtained especially using the "hybrid" density functionals[26,27] such as B3LYP and B3PW91 combining "exact exchange" with gradient-corrected density functionals. For excited states of closed shell molecules, time-dependent DFT methods (TDDFT) have been developed.[28−32] Applications of TDDFT approaches have recently begun to be reported on transition metal complexes.[33−36] In another example of a potential OLED material, the excited states of tris-(8-hydroxyquinolate)-aluminum (Alq) has been studied with TDDFT approaches.[37,38] In this paper we explore the ground and low-lying excited states of three related Ir(III) complexes Ir(ppy)$_3$ (**1**), Ir(ppy)$_2$(acac) (**2**), and Ir(ppy)$_2$(bza) (**3**) using density functional approaches techniques [where acac = acetoylacetonate and bza = benzyolacetonate]. The ground states will be treated using the B3LYP functional, and the low-lying triplet and singlet excited states will be examined using TDDFT calculations. The results will be compared to the experimental studies of the photophysical properties of this class of complexes.[5,6,10−12,14,15] The nature of the excited states, as well as the positive and negative ions with regard to "electron−hole" creation, are of relevance to their use in OLED materials.

Details of the Calculations

Calculations on the electronic ground state of Ir(ppy)$_2$(L) complexes were carried out using B3LYP density functional theory.[26,27] "Double-ζ" quality basis sets were employed for the ligands (6-31G) and the Ir (LANL2DZ). A relativistic effective core potential (ECP) on Ir[39] replaced the inner core electrons leaving the outer core [(5s)^2(5p)^6] electrons and the (5d)^6 valence electrons of Ir(III). The geometries were fully optimized without symmetry constraints. At the respective ground-state geometries, time-dependent DFT (TDDFT) calculations[28−32] using the B3LYP functional were performed. Typically the lowest 10 triplet and 10 singlet roots of the nonhermitian eigenvalue equations were obtained to obtain the vertical excitation energies. Oscillator strengths using the dipole transition matrix elements (for singlet states only). In a few cases the geometry of the lowest triplet state was examined by optimizing the structure at the unrestricted B3LYP level. The ground-state B3LYP and excited-state TDDFT calculations were carried out using Gaussian98.[40]

In addition, selected calculations were repeated using the "Stuttgart-Bonn" ECP for Ir that treats the same number of

---

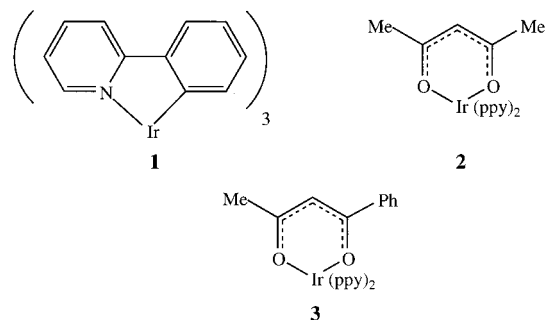* To whom correspondence should be addressed. E-mail: pjhay@lanl.gov.

Electronic States in Ir–ppy Complexes

J. Phys. Chem. A, Vol. 106, No. 8, 2002 **1635**

Figure 1. Schematic structures of *fac*-Ir(ppy)$_3$(**1**), and C-cis, N-trans isomers of Ir(ppy)$_2$(acac) (**2**) and Ir(ppy)$_2$(bza) (**3**).

valence electrons.[41] Virtually no difference was observed between the two sets of calculations. The calculated Ir-ligand bond lengths in for Ir(ppy)$_2$(acac) differed by less than 0.01 Å. TDDFT singlet and triplet excitation energies for the same complex differed by 0.01 eV.

Results

In the following sections we discuss the results of DFT calculations on the three complexes Ir(ppy)$_3$ (**1**), Ir(ppy)$_2$(acac) (**2**), and Ir(ppy)$_2$(bza) (**3**) shown in Figure 1, as well as on some other isomers. Each of the ligands (ppy = 2-phenylpyridine, acac = acetylacetonate, and bza = benzoylacetonate) is negatively charged leaving the metal in a formally 5d^6 Ir(III) state. For the calculated ground state geometries the electronic structure is examined in terms of the highest occupied and lowest virtual molecular orbitals. The properties of the positive and negative ions are also examined in this context. The nature of the low-lying excited states, which are all typically metal-to-ligand charge-transfer (MLCT) excitations, is then explored using the TD-DFT approach to derive vertical excitation energies, which are compared to existing spectroscopic data.

Ground-State Structures. The results of the optimized structures for *fac*-Ir(ppy)$_3$ (**1**), Ir(ppy)$_2$(acac) (**2**), and Ir(ppy)$_2$-(bza) (**3**) are summarized in Table 1 and shown in Figure 2. The metal–ligand bond distances are compared with X-ray diffraction studies[14,42] which have been reported for the tolylpy-ridine analogues Ir(tpy)$_3$ and Ir(tpy)$_2$(acac) of **1** and **2**, respectively, as well as the phenylpyridine complex itself Ir(ppy)$_2$-(acac) (**2**). The crystal refinements are slightly more accurate for the tpy complexes according to the quoted experimental errors. The calculated Ir–C bond lengths of 2.035 and 2.011 Å for **1** and **2**, respectively, are 0.01 Å longer than the experimental values. The Ir–N bond lengths (2.06–2.17 Å) and Ir–O bond lengths (2.19–2.20 Å) are about 0.03 and 0.05 Å longer, respectively, than the measured values. The effect of polarization functions on the six atoms bound to the Ir was examined in Ir(ppy)$_2$(acac). The resulting Ir–C (2.005 Å), Ir–N (2.059 Å), and Ir–O(2.204 Å) bond lengths differed by only −0.006, 0.000 and +0.002 Å, respectively, from the results without polarization functions.

In addition to the above complexes, which are the principal focus of these calculations and of the experimental structural and photophysical studies, we also examine alternate isomers. The *mer*-Ir(ppy)$_3$ (**4**) is also shown in Figure 2, and we also considered the "C-cis N-cis" isomers of Ir(ppy)$_2$(acac) (**5**), and Ir(ppy)$_2$(bza) (**6**), in which the strongly trans-directing Ir–C bonds are located opposite one another. The relative energies of these isomers is as follows, based on the B3LYP energies of each structure (without vibrational corrections): *mer*-Ir(ppy)$_3$ (**4**), +6.5 kcal/mol relative to **1**; "C-cis N-cis" Ir(ppy)$_2$(acac)

TABLE 1: Comparison of Calculated Bond Lengths for Ir(ppy)$_2$(L) Complexes with Experimental Values from X-ray Diffraction on the Correponding ppy or tpy (tolylpyridine) Complexes[a]

	fac-Ir(ppy)$_3$ (**1**) calcd	*fac*-Ir(tpy)$_3$ exptl[42]
R(Ir–C), Å	2.035	2.024
R(Ir–N), Å	2.167	2.132

	mer-Ir(ppy)$_3$ (**4**) calc	
R(Ir–C), Å	2.021, 2.094, 2.110	
R(Ir–N), Å	2.063, 2.080, 2.192	

	Ir(ppy)$_2$(acac) (**2**) [C-cis, N-trans] calcd	Ir(ppy)$_2$(acac) (**2**) [C-cis, N-trans] exptl[14]	Ir(tpy)$_2$(acac) exptl[14]
R(Ir–C), Å	2.011	2.003	1.982, 1.985
R(Ir–N), Å	2.059	2.010	2.023, 2.040
R(Ir–O), Å	2.202	2.146	2.136, 2.161

	Ir(ppy)$_2$(acac) (**5**) [C-cis, N-cis] calcd	
R(Ir–C), Å	2.019	
R(Ir–N), Å	2.038, 2.170	
R(Ir–O), Å	2.090, 2.191	

	Ir(ppy)$_2$(bza) (**3**) [C-cis, N-trans] calcd	
R(Ir–C), Å	2.011	
R(Ir–N), Å	2.058, 2.060	
R(Ir–O), Å	2.194, 2.196	

	Ir(ppy)$_2$(bza) (**6**) [C-cis, N-cis] calcd	
R(Ir–C), Å	2.019, 2.021	
R(Ir–N), Å	2.040, 2.171	
R(Ir–O), Å	2.087, 2.181	

[a] Typical refinement errors are 0.005 and 0.009 Å for tpy and ppy complexes, respectively.
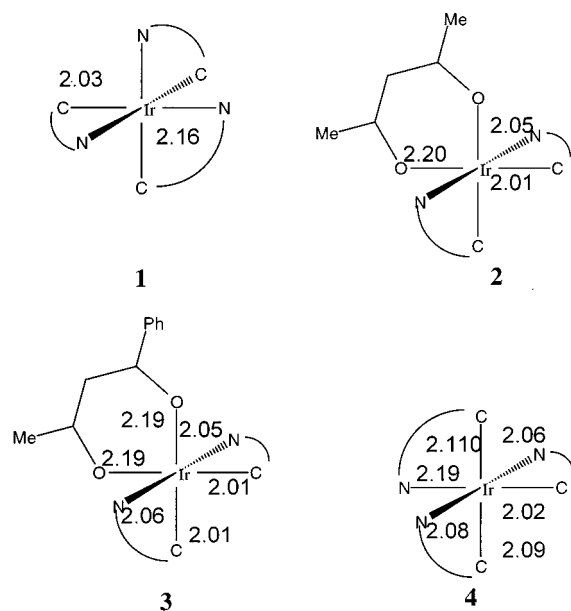

Figure 2. Calculated metal–ligand bond lengths (angstroms) from unconstrained optimizations for *fac*-Ir(ppy)$_3$(**1**), Ir(ppy)$_2$(acac) (**2**), and Ir(ppy)$_2$(bza) (**3**) and *mer*- Ir(ppy)$_3$(**4**).

(**5**), +5.3 kcal/mol relative to **2**; and "C-cis N-cis" Ir(ppy)$_2$-(bza) (**6**), +4.8 kcal/mol relative to **3**. In the unfavorable structures the Ir–N bond trans to the Ir–C bond is 0.12 Å longer than when trans to another Ir–C bond. Also the Ir–O bond shortens by about 0.12 Å when the trans Ir–C bond is replaced by Ir–N.
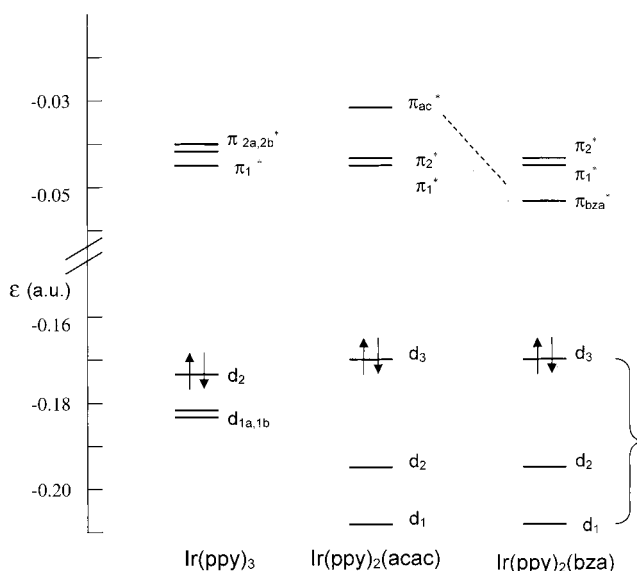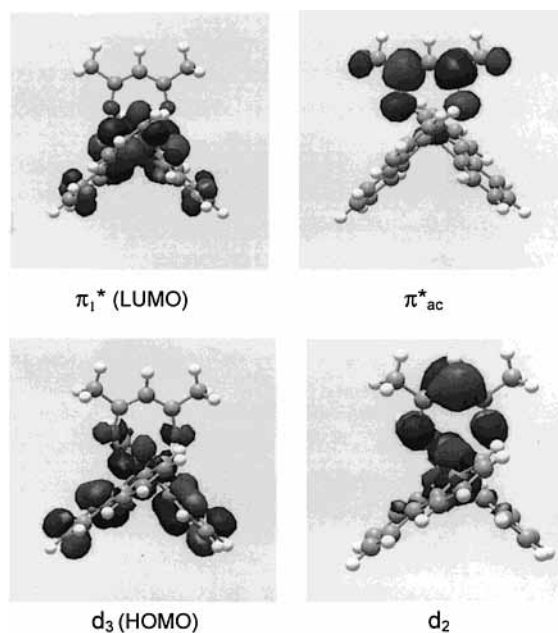
TABLE 2: Highest Occupied and Lowest Virtual Orbitals for Ir Complexes. Orbital Energies ϵ Refer to B3LYP Results. MOs on the ppy Ligands Are Numbered π_1^*, π_2^*...

designation	character Ir(ppy)$_3$	ϵ (a.u.)
occupied		
d_{1a}	5d (44%) + π(ppy)	−0.182
d_{1b}	5d (44%) + π(ppy)	−0.182
d_2	5d (52%) + π(ppy)	−0.176
virtual		
π_1^*	π(ppy)*	−0.045
π_{2a}^*	"	−0.042
π_{2b}^*	"	−0.042
	Ir(ppy)$_2$(acac)	
occupied		
d_1	5d (67%) + π(ppy)	−0.208
d_2	5d (45%) + π(ac)	−0.193
d_3	5d (45%) + π(ppy)	−0.174
virtual		
π_1^*	π(ppy)*	−0.047
π_2^*	π(ppy)*	−0.047
π_{ac}^*	π(ac)*	−0.032
	Ir(ppy)$_2$(bza)	
occupied		
d_1	5d (66%) + π(ppy)	−0.207
d_2	5d (44%) + π(bza)	−0.193
d_3	5d (45%) + π(ppy)	−0.174
virtual		
π_{bza}^*	π(bza)*	−0.053
π_1^*	π(ppy)*	−0.047
π_2^*	"	−0.046

Molecular Orbitals, Ionization Potentials and Electron Affinities. It will be useful to examine the highest occupied and lowest virtual orbitals for these Ir complexes to provide the framework for the excited state TDDFT calculations in the subsequent section. We have found that the relative ordering of the occupied and virtual orbitals provides a reasonable qualitative indication of the excitation energies, although ascribing too much meaning to individual MOs in DFT can be controversial. However, the relative orbital ordering from B3LYP results typically bears much more resemblance to experiment as compared with Hartree−Fock results. In the latter case typically the occupied d orbitals were found to lie at much lower energies compared to other orbitals, even when it is in fact the d orbitals which are the most easily ionized in photoelectron spectra or excited in electronic spectroscopy.

In each of the complexes the three highest occupied orbitals (HOMOs) correspond to the 5d manifold of Ir as might be expected for a Ir(III) d^6 complex. The orbital energies are given in Table 2 and shown schematically in Figure 3. These three highest orbitals are denoted d_1, d_2, and d_3 in most of the ensuing discussion with the exception of Ir(ppy)$_3$ where they are denoted d_{1a}, d_{1b}, and d_2 to denote the degeneracy in energy of the first two orbitals. Although the HOMO does not change in energy very much as a function of the ligand, more variation is apparent in the other 5d orbitals. This can be ascribed in part to the more weakly pi-bonding ability of the O atoms in the acac ligand compared to the ppy ligand.

While we have labeled these three highest occupied orbitals as 5d in character, there is substantial metal−ligand mixing with the pi-orbitals of the ligands. For Ir(ppy)$_3$, the resultant 5d character from population analysis is 44% for d_{1a} and d_{1b} and 52% for d_2. The lowest three LUMOs are combinations of the first π^* orbital of ppy. (In the ensuing discussion all virtual π^* orbitals will be labeled starting with π_1^* as the lowest in energy to denote orbitals on ppy ligands. When other ligands are present π^* orbitals on acac or bza will be labeled π_{ac}^* or π_{ac}^*, respectively.) For this structure with C_3 symmetry, the 3 MOs

Figure 3. Schematic drawing of orbital energies of highest occupied and lowest unoccupied MOs of Ir(ppy)$_2$(L) complexes from B3LYP calculations.

Figure 4. Contour plots of highest two occupied and lowest two virtual orbitals in Ir(ppy)$_2$(acac).

appear in an a(π_1^*) + e($\pi_{2a,2b}^*$) symmetry combination as depicted in Figure 3.

For Ir(ppy)$_3$(acac), the first two LUMOs are combinations of ppy MOs π_1^* and π_2^*, while the third lowest virtual corresponds to the acac π^* orbital π_{ac}^*. For this case a population analysis of each orbital shows the following Ir(5d) percentages: d_1 (67%), d_2 (45%), and d_3 (45%). The two highest orbitals are shown in Figure 4 in a contour plot, where the mixing of 5d and ligand π character is evident. Two of these unoccupied orbitals are also shown in Figure 4 for Ir(ppy)$_2$-(acac). The LUMO π_1^* is seen to be delocalized over the ppy ligand (and similarly for the π_2^* orbital nearly equal in energy), while the next and π_{ac}^* is delocalized on the acac ligand.

For Ir(ppy)$_2$(bza) the lowest LUMOs now corresponds to the bza π^* orbital π_{bza}^* while at slightly higher energies lie the two ppy π^* orbitals. This switch of LUMO character will play an important role in the nature of the electronic excited states discussed in the next section.

Electronic States in Ir−ppy Complexes

J. Phys. Chem. A, Vol. 106, No. 8, 2002 **1637**

TABLE 3: Energies of Positive and Negative Ions of Ir(ppy)$_2$(L) Complexes from Self-Consistent B3LYP Calculations^a

		spin density of cation		
	IP (eV)	Ir	ppy	acac/bza
Ir(ppy)$_3^+$	+5.94	0.64	0.12 (3)	
Ir(ppy)$_2$ (acac)$^+$	+5.97	0.55	0.20 (2)	0.05
Ir(ppy)$_2$ (bza)$^+$	+5.95	0.56	0.23, 0.16	0.06

		spin density of cation		
	EA (eV)	Ir	ppy	acac/ bza
Ir(ppy)$_3^-$	+0.08	−0.03	0.345 (3)	
Ir(ppy)$_2$ (acac)$^-$	+0.03	0.00	0.48, 0.42	0.10
Ir(ppy)$_2$ (bza)$^-$	+0.21	0.01	0.32, 0,12	0.54

^{a} Energies are given relative to the neutral molecule at the fixed geometry of the latter. Spin densities refer to the net atomic spin of all atoms on a given ligand.

The results of calculations on the positive and negative ions are summarized in Table 3. The IP is obtained by differences in the total self-consistent energies of the cation and the neutral ground state, and similarly for the EA. As expected by the trend in the HOMO energy, the calculated IPs of the three complexes (5.9 eV) are all relatively similar. These all correspond to removal of an electron from the "5d" orbital. As shown in the spin densities in the table, 64% of the spin density of the Ir(ppy)$_3^+$ cation is on the Ir and 12% of the density resides in π* orbitals on each ppy ligand.

All three complexes show weakly bound negative ions, corresponding to the vertical electron affinity, of ~0.1−0.2 eV. In Ir(ppy)$_3^-$ the unpaired spin density is totally on each of the ppy ligands. In Ir(ppy)$_2$(bza)$^-$ 54% of the unpaired density resides on the bza ligand, with the remainder shared on the ppy ligands. This is consistent with the LUMO being primarily the bza π* orbital. The IP and EA of these Ir complexes may be compared with tris-(8-hydroxyquinolate)-aluminum (Alq) another dopant for OLED applications. Similar DFT calculations[37] on Alq predicted 6.6 eV for the IP (vs 5.9 eV for Ir complexes) and 0.8 eV for the EA (vs ~0.1 eV for Ir complexes).

Excitation Energies. Time-dependent DFT (TDDFT) calculations[28−32] were employed to examine the low-lying triplet and singlet excited states of the Ir complexes. In this approach each excited state is written in terms of particle-hole (excitation) X_{ai} and hole-particle (deexcitation) Y_{ai} amplitudes relative to the ground-state DFT wave function.

$$|T_n\rangle = \sum_{a,i}[X_{ai}^n(P_{ia\alpha} - P_{ia\beta}) + Y_{ai}^n(P_{ai\alpha} - P_{ai\beta})]|0\rangle$$

$$|S_n\rangle = \sum_{a,i}[X_{ai}^n(P_{ia\alpha} - P_{ia\beta}) + Y_{ai}^n(P_{ai\alpha} - P_{ai\beta})]|0\rangle$$

A set of non-Hermitian equations is solved to obtain these amplitudes and the excitation energy w for each state:

$$AX + BY = wX$$

$$BY + AX = -wY$$

The larger excitation components X_{ai} correspond to the familiar occupied-to-virtual ($a \leftarrow i$) excitations P_{ia} in configuration interaction calculations. These smaller dexcitation components Y_{ai} correspond to a virtual orbital ($i \leftarrow a$) deexcitation P_{ai} from a correlated DFT solution of the ground state, $|0\rangle$.

The results from time-dependent DFT calculations (TDDFT) for Ir(ppy)$_3$ (**1**), Ir(ppy)$_2$(acac) (**2**), and Ir(ppy)$_2$(bza) (**3**), are

TABLE 4: Calculated Excitation Energies (E), Dominant Orbital Excitation, and oscillator strengths (f) from TD-DFT Calculations for Ir(ppy)$_3$^{a}

triplet states	excitation	E (eV)
T$_1$ (^{3}A)	d$_2 \rightarrow \pi_1$*	2.59
T$_2$ (^{3}E)	d$_2 \rightarrow \pi_{2a}$*	2.60
	d$_2 \rightarrow \pi_{2b}$*	2.60
T$_3$ (^{3}A)	d$_{1a,1b} \rightarrow \pi_{2a,2b}$*	2.79
T$_4$ (^{3}E)	d$_{1a} \rightarrow \pi_1$*	2.83
	d$_{1b} \rightarrow \pi_1$*	2.83
T$_5$ (^{3}E)	d$_{1a,1b} \rightarrow \pi_{2a,2b}$*	2.95
	d$_{1a,1b} \rightarrow \pi_{2a,2b}$*	2.95
T$_6$ (^{3}A)	d$_{1a,1b} \rightarrow \pi_{2a,2b}$*	2.98
T$_7$ (^{3}A)	d$_1 \rightarrow \pi_3$*	3.10

singlet states	excitation	E (eV)	f
S$_1$(^{1}A)	d$_2 \rightarrow \pi_1$*	2.80	0.0044
S$_2$ (^{1}E)	d$_2 \rightarrow \pi_{2a}$*	2.85	0.0019
	d$_2 \rightarrow \pi_{2b}$*	2.85	0.0022
S$_3$ (^{1}E)	d$_{1a} \rightarrow \pi_1$*	3.03	0.0207
	d$_{1b} \rightarrow \pi_1$*	3.04	0.0186
S$_4$ (^{1}A)	d$_{1a,1b} \rightarrow \pi_{2a,2b}$*	3.04	0.0058
S$_5$ (^{1}E)	d$_{1a,1b} \rightarrow \pi_{2a,2b}$*	3.14	0.0601
	d$_{1a,1b} \rightarrow \pi_{2a,2b}$*	3.15	0.0617
S$_6$ (^{1}A)	d$_{1a,1b}$, d$_2 \rightarrow \pi_3$*	3.18	0.0504
S$_7$ (^{1}A)	d$_{1a,1b}$, d$_2 \rightarrow \pi_3$*	3.39	0.0067

^{a} For orbital designations see Table 2.

shown in Tables 4, 5, and 6, respectively. For each molecule we typically give the vertical excitation energies for the lowest 10 triplet and singlet states calculated at the optimized structure for the ground state. The nature of the orbitals involved in the dominant excitation process is also shown, where the same convention is used from the discussion in the previous section and in Table 3 of the occupied and virtual orbitals. In some cases more than one dominant excitation process is involved for a particular state. After presenting the detailed theoretical results in this section, in the following section we summarize the excited states for the three complexes and compare to experimental absorption and emission studies.

From Table 4 we see that in Ir(ppy)$_3$ the calculated excitation energy for the lowest triplet state (T$_1$) is 2.59 eV (20800 cm^{-1}) with two higher triplet states extremely close (within 0.01 eV) in energy. All correspond to excitations from an electron in the nondegenerate HOMO with significant 5d character (d$_2$ in Table 3) to the lowest π* orbitals of the ppy ligands. In the case of T$_1$ the excitation involves the symmetric combination of the π* orbitals (^{3}A state), while the nearby states involve the e combinations of π* orbitals giving rise to a ^{3}E state overall. The corresponding singlet states are found to occur about 0.2 eV (1600 cm^{-1}) higher at 2.80 eV for S$_1$. At higher energies we find excitations from the occupied orbitals at slightly lower energy (labeled as degenerate d$_{1a}$ and d$_{1b}$) which also have significant d character.

According to this assignment we would label the lowest excited states of Ir(ppy)$_3$ as MLCT (metal-to-ligand charge transfer) states given the strong 5d component of the occupied orbital and the predominantly ligand π* virtual orbital. In fact, all of the states in Table 4 within ~0.6 eV (6000 cm^{-1}) of the lowest excited state would be characterized as MLCT states. There has been considerable discussion of the nature and relative ordering of MLCT and ligand-centered (π−π* or LC) excitations in d^6 metal complexes. As discussed in the earlier section, this analysis is complicated by the presence of strong metal−ligand mixing in the HOMO with about 50% metal 5d character in the three complexes considered here.

TABLE 5: Calculated Excitation Energies (*E*), Dominant Orbital Excitation, and Oscillator Strengths (*f*) from TD-DFT Calculations for Ir(ppy)₂(acac)

triplet states	excitation	*E* (eV)
T_1	$d_3 \rightarrow \pi_2^*$	2.47
T_2	$d_3 \rightarrow \pi_1^*$	2.48
T_3	$d_2 \rightarrow \pi_{ac}^*$	2.75
T_4	$d_2 \rightarrow \pi_2^*$	2.84
T_5	$d_2 \rightarrow \pi_1^*, d_1 \rightarrow \pi_2^*$	2.87
T_6	$d_3 \rightarrow \pi_{ac}^*$	2.99
T_7	$d_3 \rightarrow \pi_3^*$	3.09
T_8	$d_3 \rightarrow \pi_4^*$	3.14
T_9	$d_2 \rightarrow \pi_1^*, d_1 \rightarrow \pi_2^*$	3.23

singlet states	excitation	*E* (eV)	*f*
S_1	$d_3 \rightarrow \pi_2^*$	2.70	0.0314
S_2	$d_3 \rightarrow \pi_1^*$	2.73	0.0003
S_3	$d_3 \rightarrow \pi_{ac}^*$	3.05	0.0017
S_4	$d_2 \rightarrow \pi_1^*$	3.19	0.0261
S_5	$d_2 \rightarrow \pi_2^*$	3.24	0.0021
S_6	$d_3 \rightarrow \pi_3^*$	3.27	0.0296
S_7	$d_3 \rightarrow \pi_4^*$	3.36	0.0
S_8	$d_1 \rightarrow \pi_2^*$	3.56	0.0260
S_9	$d_1 \rightarrow \pi_1^*$	3.61	0.0139
S_{10}	$d_2 \rightarrow \pi_{ac}^*$	3.65	0.0175

a For orbital designations see Table 2. MOs on the ppy ligands are denoted π_1^*, π_2^*, ..., and on acac as π_{ac}^*.

TABLE 6: Calculated Excitation Energies (*E*), Dominant Orbital Excitation, and Oscillator Strengths (*f*) from TD-DFT Calculations for Ir(ppy)₂(bza)

triplet states	excitation	*E* (eV)
T_1	$d_2 \rightarrow \pi_{bza}^*$	2.42
T_2	$d_3 \rightarrow \pi_1^*$	2.48
T_3	$d_3 \rightarrow \pi_2^*$	2.49
T_4	$d_3 \rightarrow \pi_{bza}^*$	2.55
T_5	$d_2 \rightarrow \pi_1^*$	2.85
T_6	$d_2 \rightarrow \pi_2^*$	2.88
T_7	$d_3 \rightarrow \pi_3^*$	3.10
T_8	$d_1 \rightarrow \pi_{bza}^*, d_3 \rightarrow \pi_5^*$	3.14
T_9	$d_3 \rightarrow \pi_4^*, d_1 \rightarrow \pi_{bza}^*$	3.16
T_{10}	$d_1 \rightarrow \pi_1^*, d_2 \rightarrow \pi_2^*$	3.23

singlet states	excitation	*E* (eV)	*f*
S_1	$d_3 \rightarrow \pi_{bza}^*$	2.59	0.0026
S_2	$d_3 \rightarrow \pi_1^*$	2.71	0.0312
S_3	$d_3 \rightarrow \pi_2^*$	2.75	0.0006
S_4	$d_2 \rightarrow \pi_{bza}^*$	3.14	0.0314
S_5	$d_2 \rightarrow \pi_2^*$	3.22	0.0111
S_6	$d_2 \rightarrow \pi_1^*$	3.25	0.0074
S_7	$d_3 \rightarrow \pi_3^*$	3.28	0.0283
S_8	$d_3 \rightarrow \pi_4^*$	3.38	0.0006
S_9	$d_1 \rightarrow \pi_{bza}^*$	3.50	0.0928
S_{10}	$d_1 \rightarrow \pi_1^*$	3.59	0.0819

a For orbital designations see Table 2. MOs on the ppy ligands are denoted π_1^*, π_2^*..., and on bza as π_{bza}^*.

In Tables 5 and 6 we compare the results of the excited states of Ir(ppy)₂(acac) and Ir(ppy)₂(bza). From the earlier discussion of the frontier orbitals (Table 3 and Figure 3), the HOMO, a combination of Ir(5d) and ligand π orbitals, remains relatively constant in energy for all three complexes. In the case of Ir(ppy)₂(acac) the first two unoccupied orbitals are π* ppy orbitals with the π_{ac}^* lying 0.3 eV higher in energy. Accordingly we find that the lowest triplet states (T_1 and T_2) correspond to the MLCT d-π*(ppy) excitations calculated to lie at 2.47 and 2.48 eV with the corresponding lowest singlet states (S_1 and S_2) occurring at 2.70 and 2.73 eV. At 0.3 eV higher energy one finds the T_3 and S_3) states arising from the d-π_{ac}^* excitation.

TABLE 7: Properties of the Lowest Triplet States of Ir(ppy)₂(acac) Complexes from Self-consistent B3LYP Calculations. Spin Densities Refer to the Net Atomic Spin of All Atoms on a Given Ligand.

	energy (eV)	spin densities		
		Ir	ppy	acac/bza
vertical	2.64	0.57	0.65, 0.74	0.04
adiabatic (optical)	2.51			

optimized bond lengths	energy (eV)	change*a*
Ir−C	1.992	−0.019
Ir−N	2.060	+0.001
Ir−O	2.192	−0.010

a Relative to ground state.

In Ir(ppy)₂(bza) the major distinction is the lowering of the π_{bza}^* orbital, which is delocalized over the phenyl substituent ring of the parent acac, to the point where it lies slightly below the ppy orbitals π_1^* and π_2^* (Figure 3). The character of the lowest triplet state (2.42 eV) has changed and now corresponds to the MLCT d−π_{bza}^* excitation, and similarly for S_1 (2.59 eV). This contrasts with Ir(ppy)₂(acac) where the lowest triplet arose from MLCT d−π_{ppy}^*. The picture is not as straightforward, however, in that both T_1 and S_1 involve π_{bza}^*, but T_1 excites from the HOMO-1 (d_2) and S_1 excites from the HOMO (d_3). The singlet (S_2 and S_3) and triplet (T_2 and T_3) states involving the π* on the ppy, on the other hand, all behave in an analogous way to the other Ir(ppy)₂(L) complexes involving an excitation from the LUMO into the π* on the ppy ligands with a singlet−triplet splitting of about 0.3 eV.

Properties of the Lowest Triplet State in Ir(ppy)₂(acac). In addition to the previous TDDFT studies of excited states, we have examined the lowest triplet state in Ir(ppy)₂(acac) by carrying out self-consistent unrestricted B3LYP calculations both at the ground-state geometry as well as optimizing the triplet state geometry. This will provide an indication of the energy stabilization and overall geometry relaxation that occurs in the excited state in possible emission processes. The calculated T_1 SCF vertical excitation energy is 2.64 eV, which may be compared to the TDDFT excitation energy of 2.47 eV. Since higher excitations are included in TDDFT it is not surprising that a lower energy for the excited state is predicted. In Table 7 the spin densities of the triplet state are shown where there is about 0.6 unpaired electron on Ir and 0.7 unpaired electron on each ppy ligand (and almost no spin density on the acac ligand). These values are qualitatively similar to the sum of the spin densities in the positive and negative ions from Table 3.

At the optimized geometry of the triplet state (Table 7) the Ir−O and Ir−C bonds have lengthened slightly (by 0.02 and 0.01 Å, respectively) and 0.14 of energy stabilization is found, leading to an adiabatic T_1 excitation energy of 2.51 eV.

Properties of the Lowest Excited State in Other Isomers of Ir(ppy)₂(L). Finally the lowest energies of the alternate isomers (**4**−**6**) of the Ir complexes from TDDFT calculations are compared to their more stable counterparts (**1**−**3**), although at this point there is not any available experimental information on these alternate forms. We find very little difference in the absorption properties between pairs of isomers. The T_1 excitation energies are as follows: 2.52 eV for *mer*-Ir(ppy)₃ (**4**) vs 2.59 eV for *fac* (**1**); 2.52 and 2.34 eV for Ir(ppy)₂(acac) (**5**) and Ir(ppy)₂(bza) (**6**) vs 2.47 and 2.42 eV for their counterparts **2** and **3**. The corresponding S_1 singlet energies are 2.69 eV for *mer*-Ir(ppy)₃ (**4**), essentially the same as that for *fac* (**1**); 2.81 and 2.73 eV for **5** and **6** vs 2.70 and 2.59 eV for **2** and **3**.

Electronic States in Ir−ppy Complexes

J. Phys. Chem. A, Vol. 106, No. 8, 2002 **1639**

TABLE 8: Comparison of Calculated Excitation Energies (*E*) and Oscillator Strengths (*f*) for Low-lying Triplet (T$_n$) and Singlet (S$_n$) States with Experimental Data[a]

Ir(ppy)$_3$		E, eV (f) calcd	E, eV exptl[5,11]	λ, nm exptl[5,11]
T$_1$(^{3}A)	d$_2$−π_1*	2.59	2.7	450 (abs)
			2.5	500 (emis[b], ϕ > 0.4)
T$_2$(^{3}E)	d$_2$−π_2*	2.60		
T$_3$	d$_1$−π_2*	2.79	2.73	450 (emis)
S$_1$	d$_2$−π_1*	2.70 (0.004)	2.9	425
S$_3$	d$_2$−π_2*	3.03 (0.04)		
S$_5$	d$_1$−π_2*	3.15 (0.12)	3.2	380
S$_6$	d$_2$−π_3*	3.18 (0.06)		
	π−π*		4.4	280

Ir(ppy)$_2$(acac)		E, eV (f) calcd	E, eV exptl[14,15]	λ, nm exptl[14,15]
T$_1$	d$_3$−π_2*	2.47	2.49	497
			2.41	515 (emis, ϕ = 0.3)
T$_2$	d$_3$−π_1*	2.48		
T$_3$	d$_2$−π_{ac}*	2.75	2.70	460
S$_1$	d$_3$−π_2*	2.70 (0.03)		
S$_4$	d$_2$−π_1*	3.19 (0.03)	3.01	412
S$_6$	d$_3$−π_3*	3.27 (0.04)	3.59	345
S$_8$	d$_1$−π_2*	3.56 (0.03)		
	π−π*		4.76	260

Ir(ppy)$_2$(bza)		E, eV (f) calcd	E, eV exptl[14,15]	λ, nm exptl[14,15]
T$_1$	d$_2$−π_{bza}*	2.42	2.41	515 (emis, $\phi \sim$ 0.01)
T$_2$	d$_3$−π_1*	2.48		
T$_3$	d$_3$−π_2*	2.49		
S$_1$	d$_3$−π_{bza}*	2.59 (0.003)		
S$_2$	d$_3$−π_1*	2.71 (0.03)		
S$_4$	d$_2$−π_{bza}*	3.14 (0.03)		
S$_7$	d$_3$−π_4*	3.28 (0.03)		
S$_9$	d$_1$−π_{bza}*	3.50 (0.09)		
S$_{10}$	d$_1$−π_1*	3.59 (0.08)		

[a] Experimental values are from absorption spectra unless otherwise noted or emission studies. Only singlet states with appreciable oscillator strength are included (see Tables 4−6). [b] Emis = emission, ϕ = phosphorescence quantum yield.

Discussion

Comparison of Calculated Results with Experimental Studies. The results of the TDDFT calculations are compared with the experimental absorption and emission data for Ir(ppy)$_3$ (**1**), Ir(ppy)$_2$(acac) (**2**), and Ir(ppy)$_2$(bza) (**3**) as summarized in Table 8. There have been numerous spectroscopic studies on Ir(III) ppy complexes using absorption and luminescence techniques both in solution and in solid matrixes. The principal experimental studies cited in the table have been carried out by King et al.[5] and Columbo et al.[11] for Ir(ppy)$_3$ and by Thompson and co-workers[14,15] for Ir(ppy)$_2$(acac), Ir(ppy)$_2$(bza), and numerous other Ir(ppy)$_2$(L) complexes as well. The focus in our comparison will be on the lowest triplet and singlet electronic states and on the higher electronic states within ∼1 eV (8000 cm^{-1}) of the onset of absorption or emission. From the TDDFT results we have identified about the lowest 20 electronic states, but the higher electronic states probed by UV absorption studies will be beyond the scope of this initial study. For the orbital designations refer to Tables 4−6 and Figure 3.

The calculated energies correspond to vertical excitation energies at the ground state geometry which is directly comparable to measured absorption peaks. Emission bands reflect the energy differences at the excited-state geometries, on the other hand. In the next section we examine to a limited extent the effects of excited-state geometry relaxation. For the singlet−singlet excitations the calculated oscillator strengths (*f*)

are reported using the dipole approximation. Experimental absorption and emission peaks are shown as assigned to singlet or triplet states along with phosphorescence yields (ϕ) for selected triplet states.

For Ir(ppy)$_3$ the calculated excitation energy (2.59 eV) for the lowest triplet T$_1$ arising from the MLCT d$_1$−π_1* excitation is close to the onset of absorption (2.7 eV, 450 nm). Two emission bands are observed at 2.42 eV (19600 cm^{-1}) and at 2.7 eV (22000 cm^{-1}). The lower band corresponds to the T$_1$ state, and the second band agrees well with the higher T$_3$ state (^{3}E) arising from the lower occupied d orbital (d$_1$−π_1*) calculated at 2.7 eV. Experimentally this band was assigned to emission from triplet π−π* states on the ppy ligands, whereas the TDDFT results label this as another MLCT transition. This should be qualified by the fact that the "5d" orbitals are highly mixed with π character on the ligands as discussed earlier.

Higher energy absorption peaks at 2.9 eV (425 nm) and 3.2 eV (380 nm) occur in the same region of a singlet state S$_5$ calculated at 3.15 eV with large oscillator strength. The intense peak observed at 4.4 eV (283 nm) is much higher than the MLCT states found here and has been assigned to a ligand π−π* state.

The TDDFT results do not provide information on triplet−singlet absorption intensities since spin−orbit coupling effects are not included in current TDDFT approaches, which have only recently been applied to transition metal complexes. Spin−orbit coupling can mix singlet and triplet states, allowing the latter to acquire intensity in both absorption and emission. A second effect is that the triplet energies are shifted through coupling with higher singlet (or other triplet) states. For third row transition metals one estimates the lowest triplet states to be lowered by ∼0.2−0.3 eV from interactions with higher states through spin−orbit coupling. The TDDFT results should still provide a reasonable description of the overall orbital excitations that would be coupled in a subsequent spin−orbit treatment.

For Ir(ppy)$_2$(acac) the absorption at 497 nm (2.5 eV) and emission at 515 nm (2.4 eV) corresponds to the lowest calculated MLCT triplet at 2.47 eV from the highest d orbital to the ppy π* orbital. The absorption peak at 460 nm (2.7 eV) agrees well with the higher triplet state T$_3$ arising from the d$_2$−π_{ac}* excitation (2.75 eV). Alternatively the calculated S$_1$ state (2.70 eV) lies in this region, although one would expect that with spin−orbit coupling effects the singlet states would be pushed somewhat higher in energy. Higher peaks at 3.0 and 3.6 eV correspond well with the excited singlet states S$_4$ and S$_8$ at 3.2 and 3.6 eV with large oscillator strength.

We noted that a significant change occurred in the nature of the lowest unoccupied orbital in Ir(ppy)$_2$(bza), which delocalized over both the phenyl and acac regions of the bza ligand, whereas the LUMO in Ir(ppy)$_2$(acac) is on the ppy ligand. Nevertheless the close spacing of the three lowest triplet states in Ir(ppy)$_2$(bza) indicates that the splittings of the π* orbitals on ppy ligands is quite small (see Figure 3). The energy of the lowest triplet state also does not change dramatically between acac and bza, despite the qualitative change in the orbital excitation. The calculated triplet T$_1$ energy (2.42 eV) is consistent with emission observed at 515 nm (2.4 eV). A much lower phosphorescence yield (<0.01) is observed for bza compared to acac (0.3) and Ir(ppy)$_3$ (between 0.4 and 1). It is possible that the change in the nature of the lowest unoccupied orbital in bza could be responsible for the qualitative change in phosphorescence properties, but this supposition will await quantitative estimates of singlet−triplet mixing through spin−orbit coupling. Since the transitions to singlet states with large oscillator strength involve the π*

ppy orbitals, the calculated results for the bza and acac complexes are qualitatively similar.

The Nature of MLCT vs $\pi-\pi^*$ Excited States in Ir−ppy Complexes. In the previous discussion we have characterized all of the low-lying electronic states within ∼ 1 eV (∼ 8 000 cm-1) of the lowest triplet state as metal-to-ligand charge-transfer (MLCT) in character. We have also noted that the "metal" orbital ranges from 45 to 65% Ir (5d) in character, with the remainder of the orbital of ligand π character. Many luminescence studies have interpreted the results and the dependence on solvent or solid matrix as having competition between MLCT and $\pi-\pi^*$ ligand-centered (LC) states lying very close in energy. Our results indicate that at least one possible alternative interpretation is that there could be competition between different types of MLCT transitions, where one state involves a π^* orbital on the ppy ligand and another state involves a π^* orbital on the acac or bza ligand.

The contention that LC states are present in the absorption or emission spectra of Ir complexes has been made more strongly for the cationic Ir(ppy)$_2$(bpy)$^+$ species that is isoelectronic with Ir(ppy)$_3$[7−10] and the thio derivative Ir(thpy)$_3$.[9] Preliminary calculations we have performed on Ir(ppy)$_2$(bpy)$^+$ also show at least one occupied ligand-localized orbital lying between the three 5d-containing occupied orbitals found in this study of Ir(ppy)$_2$(L) complexes. Recent theoretical studies of the d^8 systems Pd(thpy)$_2$ and Pt(thpy)$_2$ found the HOMO to be a ligand-centered orbital in the sulfur-containing portion of the ring.[25]

Finally we should repeat two caveats regarding the present calculations. First the results pertain only to the ground state geometry. If there are significant geometry changes in the excited state, the luminescence properties of the complex could change significantly from the picture presented here. Our limited studies of the lowest triplet state of Ir(ppy)$_2$(acac) showed relatively little change in geometry or energy (∼0.2 eV). Second, the more detailed interpretation of effects such as phosphorescence properties will await the inclusion of spin−orbit coupling effects which are not included in these TDDFT results. We hope to investigate these effects in future studies.

Summary

The ground-state structures of the complexes Ir(ppy)$_3$ (**1**), Ir(ppy)$_2$(acac) (**2**), and Ir(ppy)$_2$(bza) (**3**) as calculated by B3LYP density functional calculations are in good agreement with available crystallographic studies. The highest occupied orbitals are Ir(5d) in character, but with almost equal admixture of ligand π orbitals. The spin densities in the cations show about 0.6 electron on the metal center, which is consistent with this analysis. The lowest virtual orbitals are totally π^* ligand in character, as also reflected in the spin densities in the anion. The nature of the lowest unoccupied orbital changes from ppy-localized to bza-localized for the series of three molecules.

Excited triplet and singlet states are examined using time-dependent density functional theory (TDDFT). All of the low-lying transitions are categorized as metal-to-ligand charge-transfer (MLCT) transitions, although the metal orbitals have significant mixture of ligand character as mentioned above. The lowest triplet state T$_1$ in Ir(ppy)$_3$ is calculated to lie at 2.59 eV compared to 2.7 eV observed in absorption and 2.5 eV in emission. For Ir(ppy)$_2$(acac) and Ir(ppy)$_2$(bza) the T$_1$ states from TDDFT are found at 2.47 eV (2.49 abs, 2.41 emis) and 2.42 eV (2.41 emis), respectively. Nearby triplet states lie within 0.1 eV and the lowest singlet states also occur within 0.1−0.2 eV. Higher peaks in absorption spectra are assigned to calculated

transitions and a higher emission band in Ir(ppy)$_3$ is consistent with a higher energy triplet state.

References and Notes

(1) Balzani, V.; Juris, A.; Venturi, M.; Campagna, S.; Serroni, S. *Chem. Rev.* **1996**, *96*, 759−833.
(2) Vlcek, A., Jr. *Coord. Chem. Rev.* **1998**, *177*, 219−256.
(3) Demadis, K. D.; Hartshorn, C. M.; Meyer, T. J. *Chem. Rev.* **2001**, *101*, 2655−2685.
(4) Demas, J. N.; DeGraff, B. A. *Coord. Chem. Rev.* **2001**, *211*, 317−351.
(5) King, K. A.; Spellane, P. J.; Watts, R. J. *J. Am. Chem. Soc.* **1985**, *107*, 1431−1432.
(6) Garces, F. O.; King, K. A.; Watts, R. J. *Inorg. Chem.* **1988**, *27*, 3464−3471.
(7) Wilde, A. P.; King, K. A.; Watts, R. J. *J. Phys. Chem.* **1991**, *95*, 629−634.
(8) Wilde, A. P.; Watts, R. J. *J. Phys. Chem.* **1991**, *95*, 622−629.
(9) Colombo, M. G.; Gudel, H. U. *Inorg. Chem.* **1993**, *32*, 3081−3087.
(10) Colombo, M. G.; Hauser, A.; Gudel, H. U. *Inorg. Chem.* **1993**, *32*, 3088−3092.
(11) Colombo, M. G.; Brunold, T. C.; Riedener, T.; Gudel, H. U.; Fortsch, M.; Burgi, H. B. *Inorg. Chem.* **1994**, *33*, 545−550.
(12) Schmid, B.; Garces, F. O.; Watts, R. J. *Inorg. Chem.* **1994**, *33*, 9−14.
(13) Neve, F.; Crispini, A.; Campagna, S.; Serroni, S. *Inorg. Chem.* **1999**, *38*, 2250−2258.
(14) Lamansky, S.; Djurovich, P.; Murphy, D.; Abdel-Razzaq, F.; Kwong, R.; Tsyba, I.; Bortz, M.; Mui, B.; Bau, R.; Thompson, M. E. *Inorg. Chem.* **2001**, *40*, 1704−1711.
(15) Lamansky, S.; Djurovich, P.; Murphy, D.; Abdel-Razzaq, F.; Lee, H. E.; Adachi, C.; Burrows, P. E.; Forrest, S. R.; Thompson, M. E. *J. Am. Chem. Soc.* **2001**, *123*, 4304−4312.
(16) Baldo, M. A.; O'Brien, D. F.; You, Y.; Shoustikov, A.; Sibley, S.; Thompson, M. E.; Forrest, S. R. *Nature* **1998**, *395*, 151−154.
(17) Baldo, M. A.; Lamansky, S.; Burrows, P. E.; Thompson, M. E.; Forrest, S. R. *Appl. Phys. Lett.* **1999**, *75*, 4−6.
(18) Adachi, C.; Baldo, M. A.; Forrest, S. R.; Thompson, M. E. *Appl. Phys. Lett.* **2000**, *77*, 904−906.
(19) Lee, C. L.; Lee, K. B.; Kim, J. J. *Appl. Phys. Lett.* **2000**, *77*, 2280−2282.
(20) Grushin, V. V.; Herron, N.; LeCloux, D. D.; Marshall, W. J.; Petrov, V. A.; Wang, Y. *Chem. Commun.* **2001**, *16*, 1494−1495.
(21) Wang, Y.; Herron, N.; Grushin, V. V.; LeCloux, D.; Petrov, V. *Appl. Phys. Lett.* **2001**, *79*, 449−451.
(22) Roos, B. O. *Acc. Chem. Res.* **1999**, *32*, 137−144.
(23) Guillaumont, D.; Daniel, C.; Vlcek, A., Jr. *Inorg. Chem.* **1997**, *36*, 1684−1688.
(24) Full, J.; Gonzales, L.; Daniel, C. *J. Phys. Chem. A* **2001**, *105*, 2595−2601.
(25) Pierloot, K.; Ceulemans, A.; Merchan, M.; Serrano-Andres, L. *J. Phys. Chem. A* **2000**, *104*, 4374−4382.
(26) Lee, C.; Yang, W.; Parr, R. G. *Phys. Rev. B* **1988**, *37*, 785.
(27) Becke, A. D. *J. Chem. Phys.* **1993**, *98*, 5648.
(28) Jamorski, C.; Casida, M. E.; Salahub, D. R. *J. Chem. Phys.* **1996**, *104*, 5134.
(29) Petersilka, M.; Grossmann, U. J.; Gross, E. K. U. *Phys. Rev. Lett.* **1996**, *76*, 1212.
(30) Bauernschmitt, R.; Ahlrichs, R.; Hennrich, F. H.; Kappes, M. M. *J. Am. Chem. Soc.* **1998**, *120*, 5052.
(31) Casida, M. E. *J. Chem. Phys.* **1998**, *108*, 4439.
(32) Stratmann, R. E.; Scuseria, G. E.; Frisch, M. J. *J. Chem. Phys.* **1998**, *109*, 8218.
(33) Rosa, A.; Baerends, E. J.; vanGisbergen, S. J. A.; vanLenthe, E.; Gooeneveld, J. A.; Snijders, J. G. *J. Am. Chem. Soc.* **1999**, *121*, 10356.
(34) Adamo, C.; Barone, V. *Theo. Chem. Acc.* **2000**, *105*, 169−172.
(35) Boulet, P.; Chermett, H.; Daul, C.; Gilardoni, F.; Rogemond, F.;

Electronic States in Ir−ppy Complexes

J. Phys. Chem. A, Vol. 106, No. 8, 2002 **1641**

Weber, J.; Zuber, G. *J. Phys. Chem. A* **2001**, *105*, 885−894.

(36) Farrell, I. R.; van Slageren, J.; Zalis, S.; Vlcek, A. *Inorg. Chim. Acta* **2001**, *315*, 44−52.

(37) Martin, R. L.; Kress, J. D.; Campbell, I. H.; Smith, D. L. *Phys. Rev. B* **2000**, *61*, 15804−15811.

(38) Halls, M. D.; Schelgel, H. B. *Chem. Mater.* **2001**, *13*, 2632−2640.

(39) Hay, P. J.; Wadt, W. R. *J. Chem. Phys.* **1985**, *82*, 299−310.

(40) Frisch, M. J.; Trucks, G. W.; Schlegel, H. B.; Scuseria, G. E.; Robb, M. A.; Cheeseman, J. R.; Zakrzewski, V. G.; Montgomery, J. A.; Stratmann, R. E.; Burant, J. C.; Dapprich, S.; Millam, J. M.; Daniels, A. D.; Kudin, K. N.; Strain, M. C.; Farkas, O.; Tomasi, J.; Barone, V.; Cossi, M.; Cammi, R.; Mennucci, B.; Pomelli, C.; Adamo, C.; Clifford, S.; Ochterski, J.; Petersson, G. A.; Ayala, P. Y.; Cui, Q.; Morokuma, K.; Malick, D. K.; Rabuck, A. D.; Raghavachari, K.; Foresman, J. B.; Cioslowski, J.; Ortiz, J. V.; Stefanov, B. B.; Liu, G.; Liashenko, A.; Piskorz, P.; Komaromi, I.; Gomperts, R.; Martin, R. L.; Fox, D. J.; Keith, T.; Al-Laham, M. A.; Peng, C. Y.; Nanayakkara, A.; Gonzalez, C.; Challacombe, M.; Gill, P. M. W.; Johnson, B. G.; Chen, W.; Wong, M. W.; Andres, J. L.; Head-Gordon, M.; Replogle, E. S.; Pople, J. A. *Gaussian 98*, revision A.9; Gaussian, Inc.: Pittsburgh, PA, 1998.

(41) Andrea, D.; Haeussermann, U.; Dolg, M.; Stoll, H.; Preuss, H. *Theor. Chem. Acta* **1990**, *77*, 123.

(42) Garces, F. O.; Dedeian, K.; Keder, N. L.; Watts, R. J. *Acta Crystallogr.* **1993**, *C49*, 1117−120.